

1 **Evaluation of Surface Microtopography Engineered by Direct Laser**
2 **Interference for Bacterial Anti-Biofouling**

3
4 Jaione Valle^{1*}, Saioa Burgui¹, Denise Langheinrich^{2,3}, Carmen Gil¹, Cristina Solano¹, Alejandro
5 Toledo-Arana¹, Ralf Helbig⁴, Andrés Lasagni^{2,3}, Iñigo Lasa^{1*}

6 _____
7
8 ¹*Laboratory of Microbial Biofilms. Instituto de Agrobiotecnología, INAMAT. Universidad*
9 *Pública de Navarra-CSIC-Gobierno de Navarra. Campus de Arrosadía. Pamplona, Spain.*

10 ²*Fraunhofer Institute for Material and Beam Technology (IWS) Dresden, Winterbergstraße 28,*
11 *01277 Dresden, Germany.*

12 ³*Institute for Manufacturing Technology, TU Dresden, George-Bähr-Straße 3c, 01069 Dresden.*

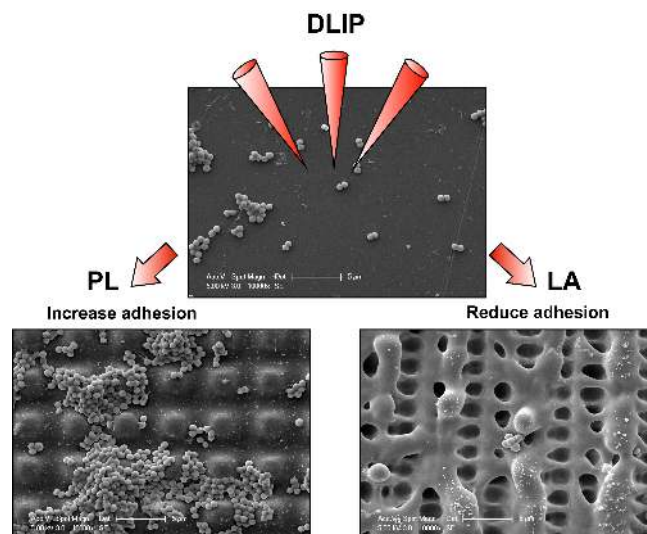
13 ⁴*Leibniz Institute of Polymer Research (IPF) Dresden, Hohe Straße 6, 01069 Dresden.*

14
15 _____
16
17
18
19
20 * Corresponding author. Jaione Valle and Iñigo Lasa.
21 Laboratory of Microbial Biofilms. Instituto de Agrobiotecnología, UPNA-CSIC. Campus de
22 Arrosadía s/n. Universidad Pública de Navarra-31006. Pamplona. Spain
23 Email: jaione.valle@unavarra.es, ilasa@unavarra.es

24

25 **Abstract**

26 Biofilm formation by bacterial pathogens on the surface of medical and industrial settings is a
27 serious health problem. Modification of the biomaterial surface topography is a promising
28 strategy to prevent bacterial attachment and biofilm development. However, fabrication of
29 functional biomaterials at large scale with periodic network-topology is still problematic. In this
30 study, we use direct laser interference **patterning** (DLIP), an easily scalable process, to modify
31 polystyrene surface (PS) topography at sub-micrometer scale. The resulting structure surfaces
32 were interrogated for their capacity to prevent adhesion and biofilm formation of the major
33 human pathogen *Staphylococcus aureus*. The results revealed that three-dimensional
34 micrometer periodic structures on PS have a profound impact on bacterial adhesion capacity.
35 Thus, line- and pillar-like topographical patterns enhanced *S. aureus* adhesion, whereas
36 complex lamella microtopography reduced *S. aureus* adhesion both in static and continuous
37 flow culture conditions. Interestingly, lamella-like textured surfaces retained the capacity to
38 inhibit *S. aureus* adhesion both when the surface is coated with human serum proteins *in vitro*
39 and when the material is implanted subcutaneously in a foreign-body associated infection
40 model. Our results establish that the DLIP technology can be used to functionalize polymeric
41 surfaces for the inhibition of bacterial adhesion to surfaces.



50 **1. Introduction**

51 One of the major challenges of **the** materials engineering discipline is to generate surfaces
52 preventing bacterial adhesion by repelling bacterial cells from attaching (antibiofouling) or
53 alternatively, inactivate the bacteria in contact with the surface (bactericidal surfaces) ^[1].
54 Colonization of the surface with bacteria has in most cases an adverse effect on the
55 functionality of the interface, such as clogging of industrial pipes and tubing, decreased
56 performance of shipping vessels, contamination of food manufacturing surfaces and medical
57 implants. The strategies to prevent and combat bacterial adhesion and proliferation to abiotic
58 surfaces include chemical modifications with antibacterial agents (antibiotics, antimicrobial
59 peptides, alkyl chains, metals, detergents) and physical modification of the surface topography
60 ^[2,3]. Because chemical modifications very often lead to toxicity due to the release of the
61 chemical compounds and rapid selection of resistant bacteria, the role of surface topography in
62 creating surfaces with antibiofouling properties is receiving greater consideration ^[4,5]. The idea
63 is to produce three-dimensional (3D) topographical patterns on the surface that result in reduced
64 contact area so that bacteria are forced to span the distance between structures to generate
65 productive interactions. Obviously, modification of the surface topography can be combined
66 with chemical coating of the surface with antibacterial agents.

67 Initial approaches to explore the effect of surface topography on bacterial adhesion were carried
68 out by mechanical roughening and polishing techniques, generating random texturized
69 roughness surfaces that modulate bacterial adhesion ^[6-11]. More recently, micropatterning
70 techniques such as optical lithography, microcontact printing, electron or ion beam lithography
71 that allow the fabrication of periodic microstructures with well-defined and reproducible
72 dimensions and shapes, have been used ^[12-16]. However, these techniques require multiple steps
73 and long processing times to produce surface geometries, especially if large areas have to be
74 processed. As a complementary alternative to these methods, the Direct Laser Interference
75 Patterning (DLIP) technology provides a new strategy to generate periodic micro- and

76 nanotopographies on different polymeric and other substrates. This method enables the large-
77 scale fabrication of complex structures by systematically varying the dimensions of the gratings
78 superimposed upon each other. Another significant advantage of DLIP compared with other
79 surface patterning methods is that fairly large areas can be processed within a short period of
80 time (up to several cm^2/s) using single or multiple laser pulses ^[17].

81 Biofilms represent the **dominant** form of bacterial life in natural environments. In biofilms,
82 bacteria grow attached to the inert surface or living tissue and embedded in an extracellular
83 matrix that protects bacteria from environmental stresses, predators, antimicrobials or the
84 immune system ^[18]. Biofilm formation starts with irreversible attachment of planktonic bacteria
85 to the surface, a process that is mediated by physical forces or specific interactions. Then,
86 sessile bacteria divide and secrete an extracellular matrix that anchors bacteria firmly to the
87 substrate and among them. Finally, single bacteria or cell clusters can actively disintegrate from
88 the biofilm or passively be shed through mechanical disruption ^[19-21]. *Staphylococcus aureus*,
89 together with *Staphylococcus epidermidis*, are the most **important Gram** positive bacterial
90 pathogens that can form biofilms on medical devices such as catheters, valves, prostheses and
91 **implantable venous access systems (port-A-caths)** ^[20-22]. *S. aureus* from skin and mucous
92 membranes from healthy humans can adhere to the surface via nonspecific interactions based
93 on the physicochemical properties of the cell envelope or through specific binding between
94 compounds of the cell envelope and proteins of the host serum coating the surface of the
95 implanted material. Living inside the biofilm increases bacterial resistance to the action of the
96 immune system and antimicrobials. As a consequence, staphylococcal biofilm associated
97 infections are difficult to eradicate and in most cases the contaminated implants need to be
98 removed to cure the infection.

99 In this study, polystyrene polymer surfaces were patterned with periodical line- (1D), pillar-like
100 (2.5D) and a complex combination of lamella- and line-like pattern (3D) by applying the Direct
101 Laser Interference Patterning (DLIP) technique. After patterning, those samples together with

102 non-patterned substrates of the same materials were used for *Staphylococcus aureus* bacterial
103 adhesion tests *in vitro* under static and continuous flow conditions as well as in an *in vivo*
104 infection model. The results revealed that line- and pillar-like patterns promote *S. aureus*
105 adhesion whereas lamella-like patterns reduce bacterial adhesion in steady state and continuous
106 flow conditions. *In vivo* testing of lamella-patterned polymers demonstrated the potential of this
107 microtopography to reduce staphylococcal biofilm on implanted materials.

108

109 **2. Experimental Section**

110 **2.1 Patterning of polymeric materials**

111 We used commercially available polymeric materials purchased from Goodfellow GmbH (Bad
112 Nauheim, Germany). Two different polystyrene (PS) substrates with a thickness of 125 μm
113 (biaxial orientated) and 1.2 mm were used. The samples were patterned using a high-power
114 pulsed, frequency quadrupled Nd:YAG laser (Quanta Ray, Spectra Physics) emitting a beam
115 with a wavelength of $\lambda = 266$ nm. The samples were irradiated with 10 ns pulses at a frequency
116 of 10 Hz. For obtaining 1D line-like structures the two beam experimental set-up was used
117 which is described elsewhere ^[23]. The spatial period Λ was varied from 1 to 5 μm by keeping a
118 constant wavelength of $\lambda = 266$ nm and varying the incident angle 2α between the two laser
119 beams following:

$$\Lambda = \frac{\lambda}{2 \sin \alpha}$$

120 For obtaining a 2D structure (e.g. pillars), the samples were rotated by an angle of 90° between
121 two subsequent laser shots. All experiments were performed at ambient conditions of pressure
122 and temperature. Polyimide (PI, Kapton HN[®]) and polyethylene terephthalate (PET) with
123 175 μm thickness were patterned using Nd:YAG laser emitting a linearly polarized beam with
124 wavelengths of $\lambda = 355$ nm (PI) and $\lambda = 266$ nm (PET).

125 **2.2 Bacterial strains and animals manipulation**

126 *S. aureus* 15981 produces high levels of b1-6 linked poly-N-acetylglucosamine (PIA/PNAG)
127 and it is accepted as a model strain of exopolysaccharide-dependent biofilm formation ^[24].
128 Staphylococci were cultured on tryptic soy agar (TSA) or broth (TSB) at 37 °C supplemented
129 with glucose (0.25 %) or with human serum (10 %) when indicated. All animal studies were
130 reviewed and approved by the Comité de Ética, Experimentación Animal y Bioseguridad, of the
131 Universidad Pública de Navarra (approved protocol PI-019/12). The work was carried out at the
132 Instituto de Agrobiotecnología under the principles and guidelines described in European
133 Directive 86/609/EEC for the protection of animals used for experimental purposes.

134 **2.3 Bacterial attachment and biofilm formation**

135 For the analysis of *S. aureus* adhesion under static conditions, an overnight culture of *S. aureus*
136 15981 strain was diluted with a ratio of 1:100. Two ml of the diluted cultured were added to 6-
137 well microtiter plate. Substrates of 2 x 2 cm² from all patterned and non-patterned (reference)
138 polymer surfaces were put in each well and plates, which were incubated for 2 hours at 37 °C
139 with shaking. After incubation, the substrates with the attached bacteria were removed from the
140 microtiter plate culture with tweezers and gently rinsed three times with sterile PBS to removed
141 non-adherent bacteria.

142 The biofilm formation under continuous flow conditions, tested on polystyrene surfaces, was
143 performed using 60-ml microfermenters (Pasteur Institute, Laboratory of Fermentation) with a
144 continuous 40 ml h⁻¹ flow of medium and constant aeration with sterile compressed air
145 (0.3 bar) ^[25]. Polystyrene wafers (1 x 1 cm²) of the patterned surfaces as well as non-patterned
146 surfaces as reference were fixed on glass slides, which were then submerged in the
147 microfermentor. Approximately 10⁸ bacteria from an overnight culture of *S. aureus* 15981 were
148 used to inoculate the microfermenters and were then kept at 37 °C for 6 h.

149 For both analyses, after incubation the substrates with the attached bacteria were removed from
150 the microtiter plate and microfermentor, respectively, gently rinsed three times with sterile PBS
151 and then placed in 1 ml of PBS and vigorously vortexed. Subsequently, the samples were

152 serially diluted and plated onto TSA plates for enumeration of viable staphylococci (colony
153 forming units, CFU). The relative adhesion was calculated as bacterial counts CFU on patterned
154 surfaces / CFU on non-patterned surfaces.

155 **2.4 Visualization and topographical characterization**

156 A scanning electron microscope (Philips XL30 ESEM-SEG) with an operating voltage of 5 kV
157 was used for visualizing the surface of the patterned sample as well as the attached bacteria. A
158 thin gold coating of several nm was sputtered on the non-conductive samples to avoid charge
159 processes. The topographical analysis (structure quality and depth) was conducted with a
160 confocal microscope (Leica DCM 3D) using a 150x objective with a lateral and z-resolution of
161 150 nm and 4 nm, respectively. For the epifluorescence analysis polystyrene wafers were
162 incubated with *S. aureus* 15981 expressing the green fluorescence protein (**GFP**) for 4 h under
163 static conditions. **Wide-field** fluorescence microscopy was used for imaging of the cells
164 attached to the PS surfaces. Each surface was visualized using a 100x oil immersion lens and 10
165 fields of view were randomly chosen for statistical analysis.

166 **2.5 *In vivo* model of polymeric-associated biofilm infection.**

167 For the *in vivo* model, patterned and non-patterned substrates with a size of 0.5 x 0.5 cm² were
168 used. Two different analyses were performed: bacterial contamination on the PS substrates (i)
169 prior and (ii) post implantation. For the prior-implantation tests, the substrates were incubated
170 with 0.5 ml of 1:100 overnight dilution of *S. aureus* 15981 culture for 1 hour at 37 °C with
171 shaking. The *in vivo* tests with post-implantation contamination were performed with sterile PS
172 substrates. For both analyses, CD1 mice (**n=6**) were anesthetized by intraperitoneal injection of
173 a ketamine/xylazine mixture. After abdominal epilation and antisepsis of the operative field, the
174 animals were operated **upon**. An incision of 1.5 cm in the skin was performed with
175 displacement of the subcutaneous space and opening of the peritoneal cavity. Then,
176 contaminated and non-contaminated respectively polymeric surfaces were fixed at the
177 abdominal wall. The peritoneal cavity was closed by suture with 6/0 Monosyn[®]. The animals

178 were put in a warm environment and when awake placed back in their cages. Within the post-
179 implantation tests, a bacterial suspension containing 10^8 bacteria of *S. aureus* 15981 was
180 injected two days after surgery intraperitoneally at the site of the polymer implantation. After 5
181 days, all animals were sacrificed and the polymeric substrates were extracted and placed in 1 ml
182 of PBS and vigorously vortexed. The samples were serially diluted and plated onto TSA plates
183 for enumeration of viable staphylococci. The relative adhesion was calculated as bacterial
184 counts CFU on patterned surfaces / CFU on non-patterned surfaces.

185 **2.6. Statistical analysis**

186 Statistical analysis was performed by one-way analysis of variance combined with the
187 Bonferroni multiple post-hoc test or by the Mann-Whitney test, with $P \leq 0.05$ considered
188 significant (GraphPad InStat, version 5).

189

190 **3. Results**

191 **3.1. Design of patterned surfaces by DLIP**

192 To analyze whether microstructures generated with Direct Laser Interference Patterning (DLIP)
193 technique on the surface of polystyrene (PS) polymers can modify bacterial adhesion capacity,
194 we generated surfaces with different microtopography geometries. We used spatial grating
195 periods (Λ) varying from 1 to 5 μm and a laser fluence that was adapted to obtain the optimal
196 structure quality (e.g. avoiding collapse of the fabricated array) depending on the spatial period
197 (Table 1). PS wafers with 1.2 mm thicknesses were patterned with periodic line (LN) and pillar
198 (PL) foils with maximal achievable structure depths of $d_{\text{Struc}} = 1.63 \pm 0.09 \mu\text{m}$ and
199 $d_{\text{Struc}} = 1.85 \pm 0.1 \mu\text{m}$ respectively (Figure 1A). Scanning electron microscopy analysis of PS
200 surfaces patterning with LN and PL revealed a well-defined, reproducible and homogeneous
201 pattern of lines and pillars with precise edges (Figure 1A and B). A similar laser treatment on
202 thin PS films (125 μm thickness) creates a combination of a lamella microtopography (LA)

203 with a 2.0 μm spatial period ($d_{\text{struc}} = 0.47 \pm 0.02 \mu\text{m}$) and a line-like structure with periodicities
204 of 6 or 8 μm ($d_{\text{struc}} = 4.33 \pm 0.06 \mu\text{m}$) (Figure 1A and B). The lamella microtopography results
205 from partially collapsing line-like features due to the lower mechanical stability of the thin PS
206 film compared to the thicker one. The results indicate that DLIP can be used to fabricate 1D to
207 3D micropatterns on PS polymers.

208 **3.2 Quantitative analysis of *S. aureus* adhesion to the patterned surfaces.**

209 The clinical strain *S. aureus* 15981 was selected to evaluate the impact of surface
210 microtopography on *S. aureus* adhesion capacity. ~~*S. aureus* 15981 produces high levels of b1-6~~
211 ~~linked poly N acetylglucosamine (PIA/PNAG) and it is accepted as a model strain of~~
212 ~~exopolysaccharide dependent biofilm formation~~^[24]. Polystyrene wafers with patterned and
213 non-patterned surfaces were incubated with bacteria in TSB-gluc media. After 2 hours, the
214 number of bacteria attached to the surface was determined by serial dilution and plating. The
215 results revealed that line- and pillar-like microtopographical patterns enhanced *S. aureus*
216 adhesion to PS polymeric materials (Figure 2A and B). In particular, a spatial period of 1 μm
217 induced higher bacterial attachment ($P < 0.05$) than periods of 5 μm . In contrast, the lamella-like
218 topography on the thin PS substrates (LA) caused a significant reduction on the adhesion of *S.*
219 *aureus* compared to non-patterned PS surfaces (CT) (Figure 2C). These results revealed that
220 microtopographical patterns on PS have a profound impact on *S. aureus* adhesion.

221

222 **3.3 Qualitative evaluation of bacterial attachment on PS polymers**

223 Because enumeration of bacteria cannot distinguish between monolayers, where most of the
224 bacteria are in contact with the surface, or scattered aggregates, where only few bacteria are in
225 contact with the surface, we used epifluorescence microscopy and scanning electron
226 microscopy to evaluate the adhesion behavior. As it is shown in Figure 3A, large aggregates of
227 bacteria attached to PL ($\Lambda = 5 \mu\text{m}$) and LN ($\Lambda = 5 \mu\text{m}$), surfaces were visualized by
228 immunofluorescence. Bacterial aggregates adhered not only to the top of the structure but also

229 inside the features. ~~These attachment patterns suggest that bacteria respond to the surface~~
230 ~~topography by maximizing the contact area with the surface.~~ In contrast, few bacteria randomly
231 oriented along the surface were attached on LA ($\Lambda=2\ \mu\text{m}$) patterned surface. Strikingly, single
232 or small aggregates of bacteria were attached to the non-modified PS surface (CT) (Figure 3A).
233 This behavior was confirmed by SEM analysis. The micrographs of patterned surfaces
234 incubated with *S. aureus* revealed large bacterial aggregates on PL polystyrene surfaces, while
235 only individual bacteria or small bacteria clusters/aggregates scattered on the surface of both
236 the LA and the non-treated materials were observed, respectively (Figure 3B).

237 **3.4 Bacterial attachment to patterned surfaces under flow-continuous conditions**

238 *S. aureus* 15981 attachment to patterned polystyrene surfaces was assessed under continuous
239 flow conditions using microfermenters^[25]. The flow rate of fresh medium ($40\ \text{ml h}^{-1}$) imposed
240 in the process was high enough to avoid any significant planktonic growth (Figure 4A).
241 Polystyrene substrates of $1\ \text{x}\ 1\ \text{cm}^2$ of PL ($\Lambda=5\ \mu\text{m}$), LA ($\Lambda=2\ \mu\text{m}$) and non-patterned surfaces
242 were fixed on the glass slides present inside the microfermenter (Figure 4B). *S. aureus* 15981
243 strain was inoculated in the microfermenters and incubated for 6 hours. In agreement with the
244 results obtained under static conditions, LA-patterned substrates significantly reduced the
245 adhesion of *S. aureus* compared to the non-patterned surfaces ($P<0.01$) (Figure 4C).
246 Furthermore, PL microtopography increased the adhesion of *S. aureus* to patterned surfaces
247 (Figure 4C).

248 Once a surface is implanted in a living body and comes into contact with biological fluids, such
249 as blood or serum, the proteins present in the media immediately coat the medical device.
250 Numerous studies indicated that coating of the medical devices with host factors may perturb *S.*
251 *aureus* attachment and biofilm formation^[1,26-28]. To address whether coating of the
252 micropatterned surface with plasma proteins has an impact on the capacity of *S. aureus* to
253 attach irreversibly to the surface, we measured the adhesion capacity of bacteria to LA
254 substrates preincubated with human serum under flow conditions. For that, LA polystyrene

255 surfaces preincubated with media supplemented with human serum (10 %) for 1 h inside the
256 microfermenter, were inoculated and incubated for 6 h with bacteria. Enumeration of the
257 bacteria attached to the LA surface revealed a small but significant decrease compared to the
258 bacteria attach to the non-patterned surface (Figure 4D). These results indicated that lamella
259 microtopography can efficiently reduce *S. aureus* adhesion under flow continuous conditions
260 even in the presence of serum proteins.

261 **3.5 *In vivo* biofilm formation model on PS surfaces**

262 Although *in vitro* assays have proven effective at identifying mechanisms involved in bacterial
263 attachment and biofilm accumulation, it is important to validate the significance of these assays
264 *in vivo*. Thus, we tested the efficacy of LA microtopography to reduce *S. aureus* attachment and
265 biofilm development using a biofilm infection model in two alternative scenarios. First, LA
266 ($\Lambda=2\ \mu\text{m}$) and control surfaces pre-coated with 10^4 CFU of *S. aureus* 15981 were implanted in
267 the intraperitoneal cavity of mice ($n=6$) (Figure 5A). After five days, animals were sacrificed, to
268 aseptically removed the polystyrene wafers and evaluate the bacterial load (Figure 5B). We
269 found that LA surfaces showed a lower degree of colonization than the non-patterned surface
270 ($P<0.05$) (Figure 5C).

271 Second, sterile LA and non-patterned PS surfaces were implanted into the mice ($n=6$) and two
272 days after surgery, contaminated with 10^8 CFU of *S. aureus* 15981. Enumeration of *S. aureus*
273 cells attached to the PS wafers 5 days after infection showed that LA surfaces displayed a
274 significantly lower colonization compared to non-patterned surfaces ($P<0.01$) (Figure 5C).
275 Thus, PS-LA wafers displayed a lower level of colonization than non-patterned PS surfaces *in*
276 *vivo*.

277

278 **4. Discussion**

279 **The establishment of multicellular communities attached to solid surfaces is one of the main**
280 **persistence strategies of bacteria in the environment, and cause serious problems in industrial**

281 settings and in medicine. Recent investigations have focused in modifying surface topography
282 as a technic to repel bacterial adhesion and biofilm formation. In this report we demonstrated
283 that DLIP technology can be used to functionalize polymeric surfaces for the inhibition of *S.*
284 *aureus* adhesion to surfaces. We showed that a lamella microtopography generated by DLIP on
285 polystyrene (PS) polymers reduced *S. aureus* adhesion both in static and continuous flow
286 culture conditions and in a foreign-body associated infection model.

287 Up to date, the methods employed for the fabrication of patterned surfaces with antibacterial
288 properties include laser writing, layer by layer self assembly (LBLSA), structural
289 transformation by electrodeposition on patterned substrates (STEPS) and lithographic
290 techniques ^[29,30]. However, these techniques present some limitations. LBLSA only allows the
291 production of disordered patterns while lithographic techniques require the used of masks that
292 can only be employed for planar surfaces fabricating patterns with relatively large feature sizes
293 ^[31]. Besides, it is difficult to implement these techniques for the treatment of large surfaces and
294 for the moment they have been used only to prepare surfaces for demonstration purposes. By
295 contrast, DLIP technology has been used to fabricate periodic structures with micrometer and
296 submicrometer patterned topography on large-area of different polymers, metals, ceramics and
297 coatings ^[23,32]. To evaluate the antiadhesion properties of the surfaces patterned with DLIP
298 technology, we have selected PS surfaces because it is a widely used biomaterial for a range of
299 medical applications, including fabrication of diagnostic instruments, medical devices,
300 implants, disposable laboratory ware and tissue culture components ^[24,33]. Our results reveal
301 that adhesion of *S. aureus* (0.6 – 1 μm) to the patterned surfaces showed that pillar (PL) and
302 line (LN) microtopographic features in the range between 1 to 5 micrometers increased
303 bacterial adhesion to not only to PS but also to PI and PET biomaterials compared with non-
304 patterned ones (Figure 2 and supplementary Figure 1). These results agree with previous
305 investigations reporting that surface features in the range of bacterium size allowed for
306 maximization of the bacteria–surface contact area, hence increasing cell attachment

307 [2,3,10,29,34,35] whereas surface with topographic features smaller than the diameter of bacterial
308 cells display a small accessible surface area [4,5,30]. In the former case, bacterial extracellular
309 appendages such as flagella, pili and fimbriae could assume the responsibility for the adhesion
310 to the sub-micrometer features [6-11,36,37]. Because *S. aureus* does not produce extracellular
311 appendages, one would predict that these bacteria would not adhere efficiently to surfaces with
312 submicrometer patterns. However, many *S. aureus* clinical strains depend on surface proteins
313 such as Bap [38], FnbB [39,40], phenol soluble modulins amyloid fibers [41] to adhere and built the
314 biofilm matrix. Thus, it cannot be excluded that some of these proteins can mediate the
315 adhesion to surfaces pattern with topographic features smaller than *S. aureus* size.

316 When laser parameters similar to those applied to PS of 1.2 mm thickness were applied on the
317 thin PS polymers (125 μm thickness), a complex topography was obtained. In this case, the first
318 irradiation process generates the characteristic 2.0 μm geometry whereas the second irradiation
319 process causes a partial collapsing of the line and creates the perpendicular lamella features.
320 This topography combines line-like patterns of 2.5 μm feature width and periodicities of 6 or
321 8 μm with lamella-like patterns of approximately 1.0 μm feature width and periodicities of 2
322 μm . So far, the LA-microtopography has only been obtained in PS polymers, though efforts are
323 being made in order to obtain the same topographic pattern on PI and PET polymers. In contrast
324 to the PL and LN microtopography, the lamella microtopography (LA) strongly inhibited
325 bacterial adhesion. The reasons why lamella microtextured reduced the capacity of *S. aureus* to
326 establish productive contacts with the surface, both under static and flow condition are not well
327 understood. It is possible that the protruded features of the topographical surface could provide
328 a physical obstacle to prevent the expansion of the bacterial clusters. For instance, physical
329 impediment seems to explain the antibacterial properties of the surface microtopographies
330 inspired in the sharkskin Sharklet AFTM. This surface comprised of topographic features
331 designed in diamond geometry (2 μm feature width and spacing, 3 μm feature height) is
332 effective at physically disrupting colonization and subsequent biofilm development [42-44].

333 Multiple studies have examined the effect of surface topography on bacterial adhesion under
334 static conditions. On the contrary, few studies have explored the effect of fluid flow on bacterial
335 attachment on engineered surfaces ^[13,24,30]. Our results using flow culture bioreactors with a
336 40 ml h⁻¹ flow rate showed that LA microtopography reduced *S. aureus* adhesion under shear
337 stress conditions significantly more effectively than in steady state conditions ^[25,30]. One
338 explanation for this observation is that the laminar fluid flow on the smooth surface creates
339 random turbulent flow due to the roughness of the micropattern surface that removes more
340 efficiently the bacteria from the surface. This effect would be amplified due to the reduction of
341 the surface area accessible to bacteria in the LA-microtopography.

342 Once a biomaterial is implanted in a living body, a layer of blood proteins or other human fluids
343 rapidly adsorbs on the surface and may alter the susceptibility of the material to inhibit bacterial
344 adhesion and biofilm formation. Studies performed *in vitro* have shown that the presence of the
345 serum proteins drastically reduce bacterial adhesion to the surface ^[26,28]. We showed that
346 lamella-like topography reduces *S. aureus* adhesion to PS surfaces in the presence of human
347 serum, though the reduction was less pronounced. Accordingly, experiments with animal
348 models showed that polystyrene surfaces with lamella microtopography reduced *S. aureus*
349 colonization and biofilm formation on PS surfaces after 5 days independently of whether the
350 infection has occurred during the surgical procedure or post-implantation. These results
351 indicated that surface microtopography showed encouraging efficacy to reduce *S. aureus*
352 attachment and biofilm development *in vivo*.

353

354 **5. Conclusions**

355 In this paper we illustrate that the flexible DLIP technology can be used to develop engineered
356 microtopographies on polystyrene polymers. The resulting microtopographies have a profound
357 impact on *S. aureus* adhesion capacity indicating that surface topography represents a

358 promising strategy to reduce *S. aureus* attachment and biofilm development on the surface of
359 indwelling medical devices.

360 However, because our knowledge about the influence of surface microtopography on bacterial
361 adhesion is still largely empirical, it is necessary to experimentally test every pattern to
362 determine its behavior under both *in vitro* and *in vivo* conditions. In our study, regular line and
363 pillar-like patterns enhance *S. aureus* adhesion whereas a irregular lamella microtopography
364 reduces adhesion both in static and continuous flow culture conditions. **Moreover, lamella-like**
365 **textured surfaces inhibit *S. aureus* adhesion in the presence of human serum proteins and when**
366 **the material is implanted subcutaneously in a foreign-body associated infection model strongly**
367 **suggesting that polystyrene surfaces composed of lamella-like texture might provide a**
368 **promising strategy to reduce *S. aureus* adhesion to biomedical surfaces.** Ongoing research is
369 necessary to demonstrate that lamella microtopography on the surface of other polymers, such
370 as polyimide and poly(ethylene terephthalate), also inhibits *S. aureus* adhesion.

371

372 **Acknowledgements**

373 J. Valle was supported by Spanish Ministry of Science and Innovation “Ramón y Cajal”
374 contract. This research was supported by grants AGL2011-23954 and BIO2011-30503-C02-02
375 from the Spanish Ministry of Economy and Competitiveness and IIQ14066.RI1 from Innovation
376 Department of the Government of Navarra. A. Lasagni, D. Langhenrich and R. Helbig thank
377 the Deutsche Forschungsgemeinschaft (DFG) for the financial support of the project
378 “Mechanically stable anti-adhesive polymer surfaces” (LA-2513 4-1).

379 **References**

- 380 [1] J. Hasan, R.J. Crawford, E.P. Ivanova, *Trends Biotechnol.* **2013**, *31*, 295.
381 [2] M.L.W. Knetsch, L.H. Koole, *Polymers* **2011**, *3*, 340.
382 [3] S.R. Shah, A.M. Tataru, R.N. D'Souza, A.G. Mikos, F.K. Kasper, *Materials Today*
383 **2013**, *16*, 177.
384 [4] P. Basak, B. Adhikari, I. Banerjee, T.K. Maiti, *J Mater Sci Mater Med* **2009**, *20 Suppl*
385 *1*, S213.
386 [5] I. Francolini, L. D'Ilario, E. Guaglianone, G. Donelli, A. Martinelli, A. Piozzi, *Acta*
387 *Biomater* **2010**, *6*, 3482.
388 [6] S. Abban, M. Jakobsen, L. Jespersen, *Food Microbiol.* **2012**, *31*, 139.
389 [7] R.D. Boyd, J. Verran, M.V. Jones, M. Bhakoo, *Langmuir* **2002**, *18*, 2343.
390 [8] N. Mitik-Dineva, J. Wang, V.K. Truong, P. Stoddart, F. Malherbe, R.J. Crawford, E.P.
391 Ivanova, *Curr. Microbiol.* **2009**, *58*, 268.
392 [9] B. Park, V. Nizet, G.Y. Liu, *J Bacteriol* **2008**, *190*, 2275.
393 [10] K.A. Whitehead, J. Verran, *Food Bioprod Process* **2006**, *84*, 253.
394 [11] K.A. Whitehead, D. Rogers, J. Colligon, C. Wright, J. Verran, *Colloid Surface B* **2006**,
395 *51*, 44.
396 [12] A. Biswas, I.S. Bayer, A.S. Biris, T. Wang, E. Dervishi, F. Faupel, *Adv Colloid*
397 *Interface Sci* **2012**, *170*, 2.
398 [13] M.V. Graham, A.P. Mosier, T.R. Kiehl, A.E. Kaloyeros, N.C. Cady, *Soft Matter* **2013**,
399 *9*, 6235.
400 [14] M. Graham, N. Cady, *Coatings* **2014**, *4*, 37.
401 [15] P. Kim, A.K. Epstein, M. Khan, L.D. Zarzar, D.J. Lipomi, G.M. Whitesides, J.
402 Aizenberg, *Nano Lett.* **2012**, *12*, 527.
403 [16] K. Manabe, S. Nishizawa, S. Shiratori, *ACS Appl Mater Interfaces* **2013**, *5*, 11900.
404 [17] M. Bieda, C. Schmädicke, T. Roch, A. Lasagni, *Adv. Eng. Mater.* **2014**, n.
405 [18] J.W. Costerton, P.S. Stewart, E.P. Greenberg, *Science* **1999**, *284*, 1318.
406 [19] G. O'Toole, H.B. Kaplan, R. Kolter, *Annu Rev Microbiol* **2000**, *54*, 49.
407 [20] L. Hall-Stoodley, P. Stoodley, *Curr Opin Biotechnol* **2002**, *13*, 228.
408 [21] L. Hall-Stoodley, P. Stoodley, *Trends Microbiol* **2005**, *13*, 7.
409 [22] F. Götz, *Curr Opin Microbiol* **2004**, *7*, 477.
410 [23] D. Langheinrich, E. Yslas, M. Broglia, V. Rivarola, D. Acevedo, A. Lasagni, *J. Polym.*
411 *Sci. B Polym. Phys.* **2011**, *50*, 415.
412 [24] J. Valle, A. Toledo-Arana, C. Berasain, J.-M. Ghigo, B. Amorena, J.R. Penadés, I.
413 Lasa, *Mol Microbiol* **2003**, *48*, 1075.
414 [25] J.M. Ghigo, *Nature* **2001**, *412*, 442.
415 [26] D. Campoccia, L. Montanaro, H. Agheli, D.S. Sutherland, V. Pirini, M.E. Donati, C.R.
416 Arciola, *Int J Artif Organs* **2006**, *29*, 622.
417 [27] T.J. Foster, J.A. Geoghegan, V.K. Ganesh, M. Höök, *Nat Rev Micro* **2014**, *12*, 49.
418 [28] J.D. Patel, M. Ebert, R. Ward, J.M. Anderson, *J Biomed Mater Res Part A* **2007**, *80*,
419 742.
420 [29] K.A. Whitehead, J. Colligon, J. Verran, *Colloid Surface B* **2005**, *41*, 129.
421 [30] L.-C. Xu, C.A. Siedlecki, *Acta Biomater* **2012**, *8*, 72.
422 [31] A. Komaromy, R.I. Boysen, H. Zhang, I. McKinnon, F. Fulga, M.T.W. Hearn, D.V.
423 Nicolau, *Microelectron Eng* **2009**, *86*, 1431.
424 [32] A.S.F. Lasagni, D. Langheinrich, S. Eckhardt **2012**, Plastic Research Online.
425 [33] K. Modjarrad, S. Ebnesajjad *Handbook of Polymer Applications in Medicine and*
426 *Medical Devices*, Amsterdam : Elsevier/William Andrew, **2013**
427 [34] M. Katsikogianni, Y.F. Missirlis, *Eur Cell Mater* **2004**, *8*, 37.
428 [35] A.Z. Komaromy, S. Li, H. Zhang, D.V. Nicolau, R.I. Boysen, M.T.W. Hearn,
429 *Microelectron Eng* **2012**, *91*, 39.

- 430 [36] L.C. Hsu, J. Fang, D.A. Borca-Tasciuc, R.W. Worobo, C.I. Moraru, *Appl Environ*
431 *Microbiol* **2013**, *79*, 2703.
- 432 [37] R.S. Friedlander, H. Vlamakis, P. Kim, M. Khan, R. Kolter, J. Aizenberg, *Proc Nat*
433 *Acad Sci USA* **2013**.
- 434 [38] C. Cucarella, C. Solano, J. Valle, B. Amorena, I. Lasa, J.R. Penadés, *J Bacteriol* **2001**,
435 *183*, 2888.
- 436 [39] M. Vergara-Irigaray, J. Valle, N. Merino, C. Latasa, B. García, I. Ruiz de Los Mozos,
437 C. Solano, A. Toledo-Arana, J.R. Penadés, I. Lasa, *Infect and Immun* **2009**, *77*, 3978.
- 438 [40] E. O'Neill, C. Pozzi, P. Houston, H. Humphreys, D.A. Robinson, A. Loughman, T.J.
439 Foster, J.P. O'Gara, *J Bacteriol* **2008**, *190*, 3835.
- 440 [41] K. Schwartz, A.K. Syed, R.E. Stephenson, A.H. Rickard, B.R. Boles, *PLoS Pathog*
441 **2012**, *8*, e1002744.
- 442 [42] K.K. Chung, J.F. Schumacher, E.M. Sampson, R.A. Burne, P.J. Antonelli, A.B.
443 Brennan, *Biointerphases* **2007**, *2*, 89.
- 444 [43] J.F. Schumacher, M.L. Carman, T.G. Estes, A.W. Feinberg, L.H. Wilson, M.E. Callow,
445 J.A. Callow, J.A. Finlay, A.B. Brennan, *Biofouling* **2007**, *23*, 55.
- 446 [44] J.F. Schumacher, C.J. Long, M.E. Callow, J.A. Finlay, J.A. Callow, A.B. Brennan,
447 *Langmuir* **2008**, *24*, 4931.
448

449 **Table 1. Description of polymeric materials modified by DLIP**

450

451

452

453

454

455

456

457

458

459

460

461

Polymeric material	Λ = period (μm)	Topography	F = Fluence (J/cm^2)
PS	5	Line (LN)	0.5
PS	5	Pillar (PL)	0.5
PS	3	Line (LN)	0.5
PS	3	Pillar (PL)	0.5
PS	1	Line (LN)	0.5
PS	1	Pillar (PL)	0.5
PS	5	Lamella (LA)	0.5
PS	2	Lamella (LA)	0.5
PS	-	Non-patterned (CT)	-

462

463

464

465

466

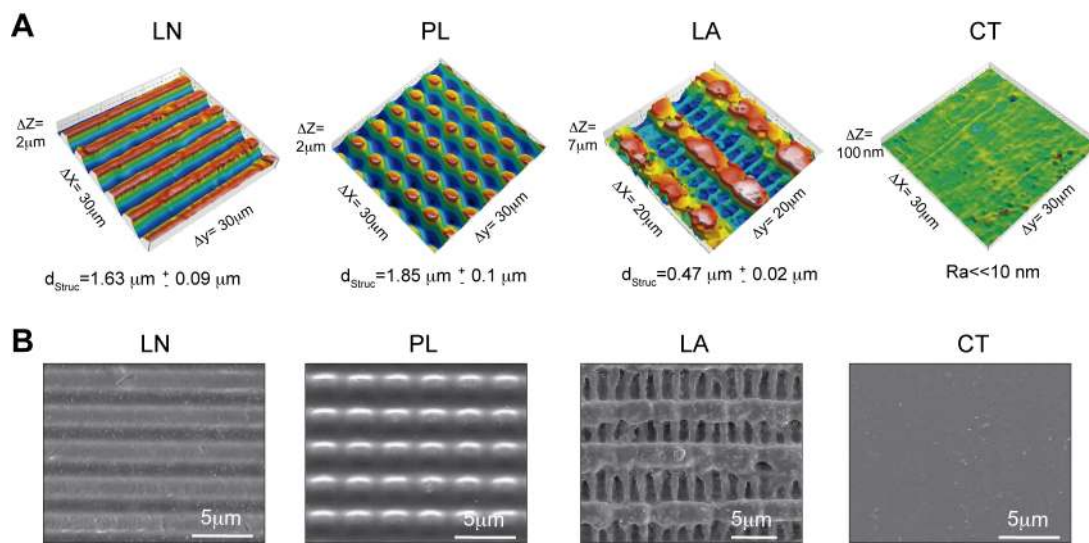
467

468

469

470

471



472 **Figure 1:** Images from confocal (A) and scanning electron microscopy (B) of PS polymeric
473 surfaces structured by Direct Laser Interference Patterning technique. Periodic arrays of line-
474 like (LN, $\Lambda = 5 \mu\text{m}$), pillar-like (PL, $\Lambda = 5 \mu\text{m}$), lamella-like (LA, $\Lambda = 2 \mu\text{m}$) structures and
475 non-modified surfaces (CT). The laser fluence was kept constant at 0.5 J cm^{-2} .

476

477

478

479

480

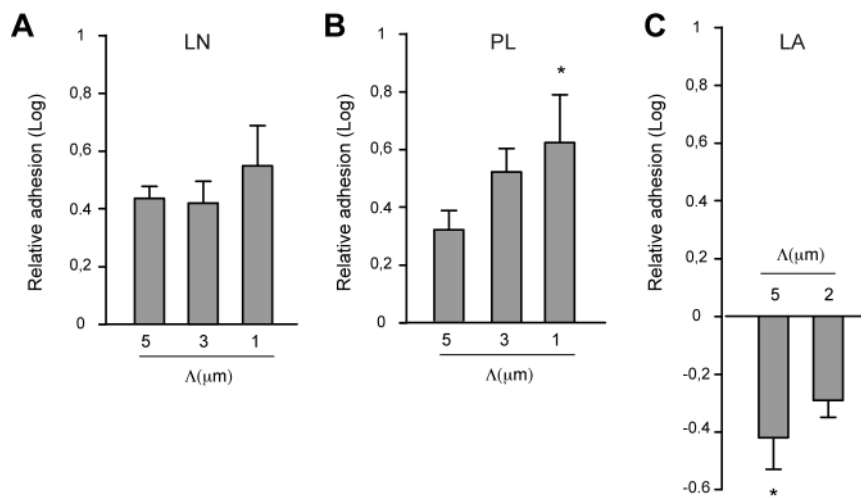
481

482

483

484

485



486 **Figure 2.** Bacterial adhesion on patterned surfaces under static conditions. Relative adhesion of
487 *S. aureus* on PS patterned surfaces with line (LN) (A), pillar (PL) (B), and lamella-like (LA)
488 (C) structures and with spatial periods (Λ) of 1, 2, 3 and 5 μm . Relative adhesion was
489 calculated as bacterial counts CFU on patterned surfaces / CFU on non-patterned surfaces.
490 Multiple comparisons were performed by one-way analysis of variance combined with the
491 Bonferroni multiple comparison test (GraphPad Instat, version 5). Asterisk indicates significant
492 adhesion differences (*, $P < 0.05$ [significant]). ns, non significant differences.

493

494

495

496

497

498

499

500

501

502

503

504

505

506

507

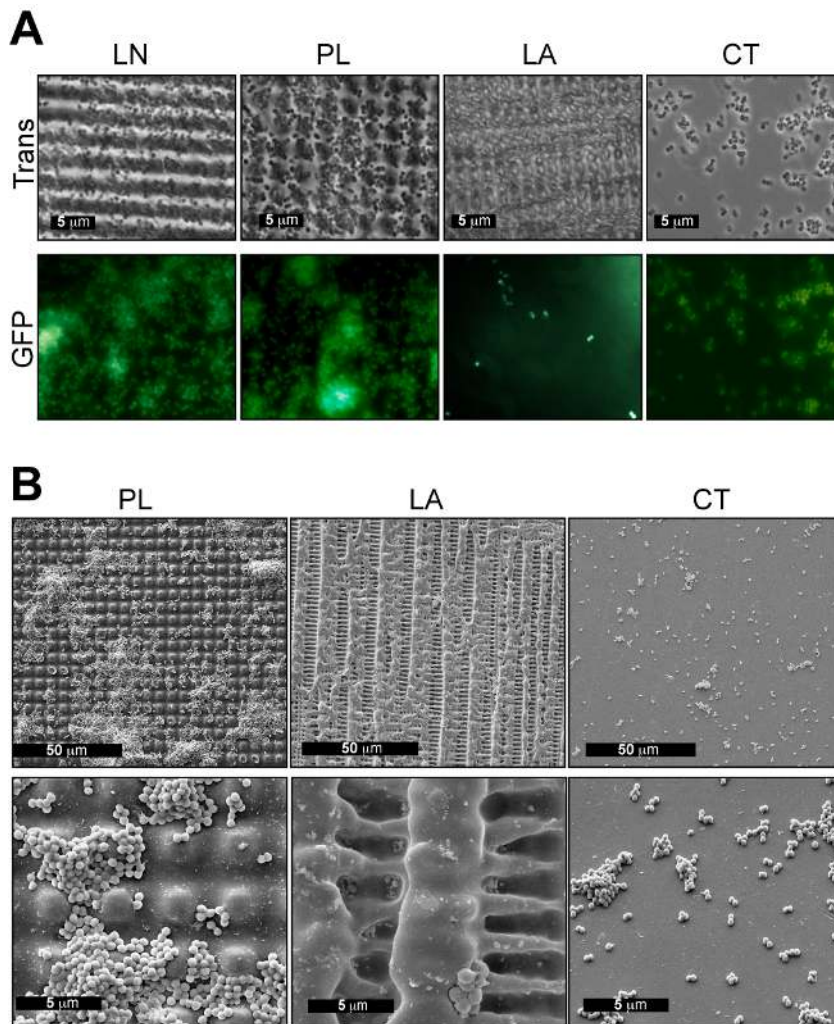
508 **Figure 3:** Qualitative evaluation of *S. aureus* attachment to patterned PS wafers. A)

509 Fluorescence microscopic images of *S. aureus* 15981-GFP attached to PL ($\Lambda=5\ \mu\text{m}$), LN ($\Lambda=5$

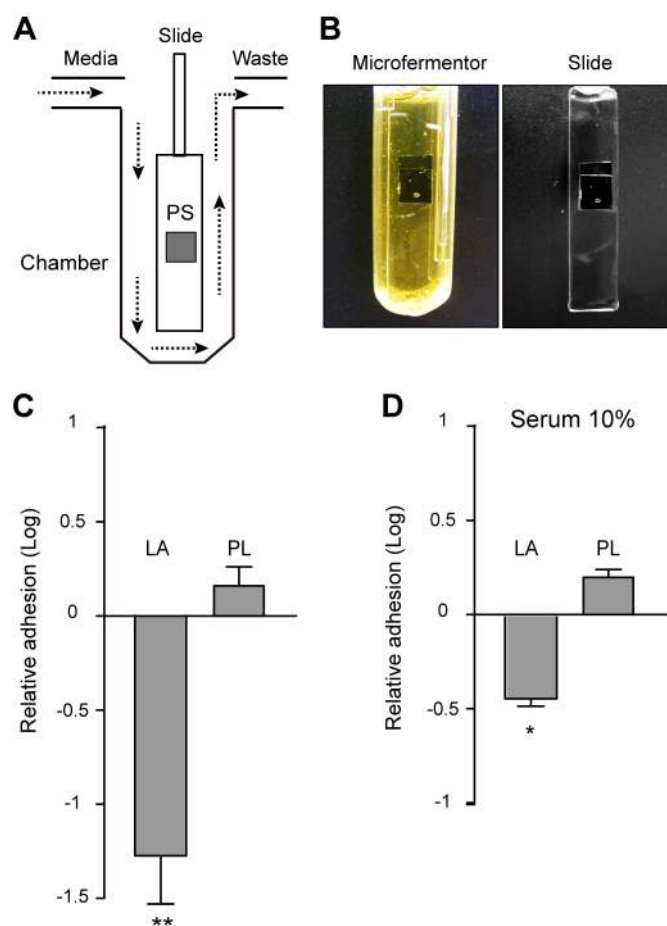
510 μm), LA ($\Lambda=2\ \mu\text{m}$), and non-patterned PS surfaces (CT), showing that bacteria respond to the

511 surface topography. B) Scanning electron micrographs of *S. aureus* cells attached to PL, LA

512 and non-patterned PS surfaces (CT).



513
514
515
516
517
518
519
520
521
522
523
524
525



526 **Figure 4:** Bacterial adhesion on patterned surfaces in microfermenters. Schematic diagram (A)
527 and photograph image taken from the microfermenters (B). Substrates of 1x1 cm² were fixed on
528 the glass slide. Microfermenters were inoculated with *S. aureus* 15981 (OD_{600nm}=1). After 6
529 hours of incubation, substrates were removed from the glass slide and quantification of adhered
530 *S. aureus* cells was performed by CFU counting of the bacteria removed from the tested
531 surfaces. Graphs show the relative adhesion of *S. aureus* on LA ($\Lambda=2\ \mu\text{m}$), PL ($\Lambda=5\ \mu\text{m}$) and
532 non-patterned (CT) PS surfaces under flow culture conditions in the absence (C) or presence of
533 human serum (D). Relative adhesion was calculated as bacterial counts CFU on patterned
534 surfaces / CFU on non-patterned surfaces. Comparisons were performed by one-way analysis of
535 variance combined with the Bonferroni multiple comparison test or Mann-Whitney test
536 (GraphPad InStat, version 5)

537

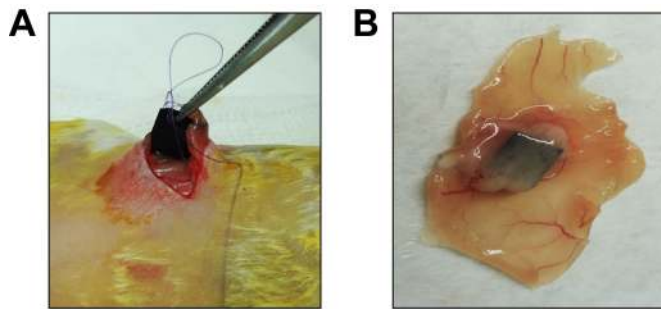
538

539

540

541

542



543

544

545

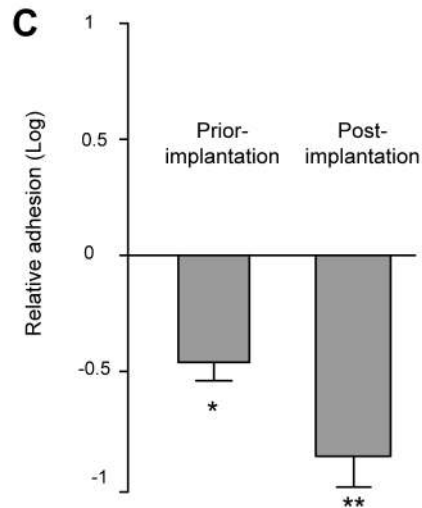
546

547

548

549

550



551 **Figure 5:** Biofilm formation of *S. aureus* on lamella-like patterned surfaces using an *in vivo*

552 model. A) Implantation of substrates in the intraperitoneal cavity of CD1 mice. B) Biofilm-

553 infected surfaces after 5 days of infection. C) Contamination of PS polymers prior-

554 implantation: PS lamella-like ($\Lambda=2\ \mu\text{m}$) and control surfaces were first coated with 10^4 cfu of *S.*

555 *aureus* 15981 and then fixed at the abdominal wall. Contamination of PS polymers post-

556 implantation: PS polymers were first fixed at the abdominal wall before infection. Two day

557 after implantation a 10^8 cfu of *S. aureus* 15981 were injected intraperitoneally at the site of the

558 implant. After 5 days, animals (n=6) of both types of infections were sacrificed and substrates

559 were extracted and placed in 1 ml of PBS. Samples were serially diluted and plated onto TSA

560 plates for enumeration of viable staphylococci.

561

562

563